Reflective tilted fiber Bragg grating refractometer based on strong cladding to core recoupling

Tuan Guo,[1,*] Hwa-Yaw Tam,[1] Peter A. Krug,[2] and Jacques Albert[2]

[1] Photonics Research Center, Department of Electrical Engineering, The Hong Kong Polytechnic University, Kowloon, Hong Kong SAR, China

[2] Department of Electronics, Carleton University, 1125 Colonel By Drive, Ottawa, Ontario K1S 5B6, Canada

[*]Corresponding author: guotuan2001@163.com

Abstract: A novel in-fiber structure for power-referenced refractometry with the capability to measure surrounding refractive index (SRI) as low as 1.33 is proposed and demonstrated. A short optical fiber stub containing a weakly tilted Bragg grating is spliced to another fiber with a large lateral offset. The reflection from this structure occurs in two well-defined wavelength bands, the Bragg reflected core mode and the cladding modes. The cladding modes reflect different amounts of power as the SRI changes, while the core-mode reflection from the same weakly tilted FBG remains unaffected by the SRI. The power reflected in the core mode band can be used as a reliable reference to cancel out any possible power fluctuations. The proposed refractometer with improved sensitivity for low SRI measurement together with the tip-reflection sensing feature, is a good candidate for sensing in chemical and biological applications.

©2009 Optical Society of America

OCIS codes: (060.2370) Fiber optics sensors; (060.0060) Fiber optics and optical communications.

References and links

1. Y. Y. Shevchenko and J. Albert, "Plasmon resonances in gold-coated tilted fiber Bragg gratings," Opt. Lett. **32**, 211-213 (2007).
2. T. Allsop, R. Neal, S. Rehman, D. J. Webb, D. Mapps, and I. Bennion, "Generation of infrared surface plasmon resonances with high refractive index sensitivity utilizing tilted fiber Bragg gratings," Appl. Opt. **46**, 5456-5460 (2007).
3. W. Liang, Y. Y. Huang, Y. Xu, R. K. Lee, and A. Yariv, "Highly sensitive fiber Bragg grating refractive index sensors," App. Phys. Lett. **86**, 151-122 (2005).
4. X. F. Chen, K. M. Zhou, L. Zhang, and I. Bennion, "Optical chemsensor based on etched tilted Bragg grating structures in multimode fiber," IEEE Photon. Technol. Lett. **17**, 664-666 (2005).
5. A. N. Chryssis, S. M. Lee, S. B. Lee, S. S. Saini, and M. Dagenais, "High sensitivity evanescent field fiber Bragg grating sensor," IEEE Photon. Technol. Lett. **17**, 1253-1255 (2005).
6. A. Iadicicco, A. Cusano, S. Campopiano, A. Cutolo, and M. Giordano, "Thinned fiber Bragg gratings as refractive index sensors," IEEE Sens. J. **5**, 1288-1295 (2005).
7. M. C. P. Huy, G. Laffont, Y. Frignac, V. Dewynter-Marty, P. Ferdinand, P. Roy, J. M. Blondy, D. Pagnoux, W. Blanc, and B. Dussardier, "Fibre Bragg grating photowriting in microstructured optical fibres for refractive index measurement," Meas. Sci. Technol. **17**, 992-997 (2006).
8. M. C. P. Huy, G. Laffont, V. Dewynter, P. Ferdinand, P. Roy, J. Auguste, D. Pagnoux, W. Blanc, and B. Dussardier, "Three-hole microstructured optical fiber for efficient fiber Bragg grating refractometer," Opt. Lett. **32**, 2390-2392 (2007).
9. M. C. P. Huy, G. Laffont, V. Dewynter, P. Ferdinand, L. Labonté, D. Pagnoux, P. Roy, W. Blanc, and B. Dussardier, "Tilted Fiber Bragg Grating photowritten in microstructured optical fiber for improved refractive index measurement," Opt. Express **14**, 10360-10370 (2006).
10. G. Laffont and P. Ferdinand, "Tilted short-period fibre-Bragg-grating-induced coupling to cladding modes for accurate refractometry," Meas. Sci. Technol. **12**, 765-770 (2001).
11. C. F. Chan, C. Chen, A. Jafari, A. Laronche, D. J. Thomson, and J. Albert, "Optical fiber refractometer using narrowband cladding-mode resonance shifts," Appl. Opt. **46**, 1142-1149 (2007).

12. M. Kežmah and D. Đonlagic´, "Multimode all-fiber quasi-distributed refractometer sensor array and cross-talk mitigation," Appl. Opt. **46**, 4081-4091 (2007).
13. H. J. Patrick, A. D. Kersey, and F. Bucholtz, "Analysis of the response of long period fiber gratings to external index of refraction," J. Lightwave Technol. **16**, 1606-1612 (1998).
14. I. D. Villar, I. R. Matias, and F. J. Arregui, "Enhancement of sensitivity in long-period fiber gratings with deposition of low-refractive index materials," Opt. Lett. **30**, 2363-2365 (2005).
15. L. Rindorf and O. Bang, "Highly sensitive refractometer with a photonic-crystal-fiber long-period grating," Opt. Lett. **33**, 563-565 (2008).
16. Q. Wang and G. Farrell, "All-fiber multimode-interference-based refractometer sensor: proposal and design," Opt. Lett. **31**, 317-319 (2006).
17. C. A. Barrios, K. B. Gylfason, B. Sánchez, A. Griol, H. Sohlström, M. Holgado, and R. Casquel, "Slot-waveguide biochemical sensor," Opt. Lett. **32**, 3080-3082 (2007).
18. F. Xu, V. Pruneri, V. Finazzi, and G. Brambilla, "An embedded optical nanowire loop resonator refractometric sensor," Opt. Express **16**, 1062-1067 (2008).
19. T. Guo, C. Chen, A. Laronche, and J. Albert, "Power-referenced and temperature-calibrated optical fiber refractometer," IEEE Photon. Technol. Lett. **20**, 635-637 (2008).
20. T. Guo, A. Ivanov, C. Chen, and J. Albert, "Temperature-independent tilted fiber grating vibration sensor based on cladding-core recoupling," Opt. Lett. **33**, 1004-1007 (2008).

1. Introduction

Most kinds of optical fiber and waveguide refractometers work through the perturbation of modal effective indices induced by changes in the surrounding refractive index (SRI) [1-19]. Such perturbations are optically detected using either the resonance wavelength shifts of short- or long-period grating devices [1-15], or the fringe shifts of interferometric devices, most commonly of the Mach-Zehnder and ring resonator types [16-18]. One of the issues associated with such devices is that in order for the perturbation to be large, i.e. for the refractometer to be sensitive, the modal field considered must overlap strongly with the region where refractive index changes are to be measured. In practice, it means that the highest sensitivity is achieved when the modes involved in the measurement are close to their wavelength cut-off point and hence extend far outside of their waveguiding layers. Because of this, most types of glass fiber refractometers reported so far achieve their highest sensitivities for SRI values larger than 1.4, i.e. for indices that are approaching that of the glass guiding media. However, there are many important applications for refractometers that operate in water or water-based solutions (including most biological and many environmental applications) where the SRI values are significantly lower, near 1.33 at optical wavelengths. Suggested solutions to address this problem include the use of very thin high index coatings (i.e. excitation of surface plasmon resonances at the external surface of the gold or silver film along the fiber) [1-2], reducing the size of the waveguiding structures to approach cut-off at lower values of SRI [3-6], microstructured or photonic-crystal fiber based gratings [7-9,15] or finding ways to access very high order modes in multimode structures (such as cladding modes of conventional single core mode fibers) [10-12].

In the work presented here, we propose and demonstrate a variant of the last approach that is particularly simple to implement and that does not require wavelength sensitive measurements. The device uses the combination of a tilted fiber Bragg grating (TFBG) with a core offset splice in a single mode optical fiber (Fig. 1). We have shown earlier that refractometric information is contained in the total power transmitted through a TFBG [19], because the transmission spectrum shape changes with SRI as was originally demonstrated by Laffont and Ferdinand [10]. However the dynamic range of that device is rather limited and the sensitivity drops rapidly for SRI values below 1.4. In the new configuration shown here, the core offset splice is used to re-couple the cladding modes generated by the TFBG into the guided core mode, similar to our recently demonstrated vibration sensor [20], but with a much larger lateral offset splice to ensure the re-coupling of high order cladding modes. The measurement is now carried out in reflection and results in a large increase in dynamic range, and most importantly, we will show that the sensitivity can be greatly enhanced in desirable SRI ranges (1.33 to 1.40) by bandpass filtering the reflected power. In comparison to long-period grating devices, a single grating design based on TFBG can be used for many different

applications since a large number of closely separated cladding modes are generated by one grating. The temperature sensitivity of TFBG is low and constant with a typical resonance shift of only ~10 pm/°C, which is similar to the core mode (Bragg resonance) at their longer wavelength side.

2. Sensor design and fabrication

Figure 1 shows our new sensing scheme. The basic idea in this configuration is to re-capture backward propagating cladding modes into the fiber core as efficiently as possible via a laterally misaligned fused splice located a short distance upstream of the TFBG. In general, the backward transmitted cladding modes emitted from the tilted grating planes can not propagate for a long distance along the fiber cladding due to the absorption of the high-index jacket material. However, when the fiber is kept straight and the cladding is not covered by absorbing material, many modes can propagate for several centimeters without much loss. Unlike the low order cladding modes which propagate close to the core/cladding boundary, the backward transmitted high order cladding modes are extremely sensitive to the outer cladding/surrounding boundary but their reflected power is very small. Therefore, to ensure an effective recoupling of higher order cladding modes, keeping a short distance between the splicing point and a downstream TFBG is necessary. In our experiment, the gap distance is set at 3 mm.
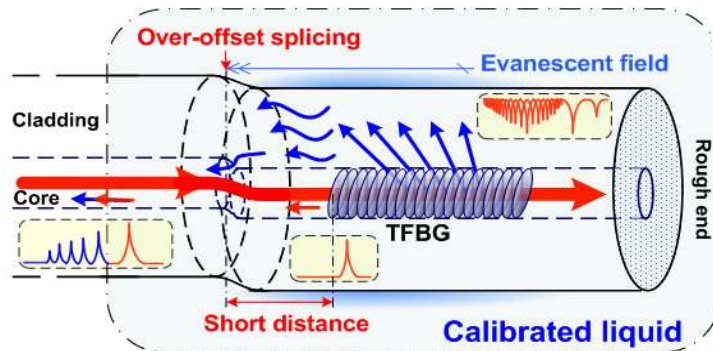

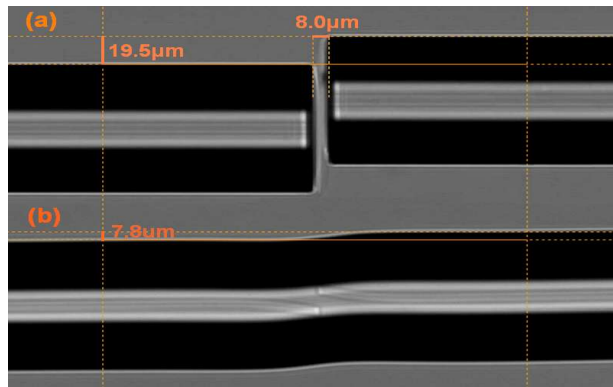Fig. 1. Schematic diagram of over-offset TFBG refractometer

Fig. 2. Photographs of the over-offset splicing process (a) 19.5 μm pre-offset before splicing and (b) 7.8 μm core-core misalignment after splicing

The lateral-offset splicing is performed by a Vytran GPX-3400 glass processing system. It incorporates a filament "furnace" assembly which provides a stable high-temperature heat source for precise control of fiber processing conditions. The heat source inside is an "omega" shaped tungsten resistive filament loop with a diameter of 900 μm and width of 625 μm. The fiber stub containing the TFBG and the connecting fibre are precisely positioned using

stepper-motor-controlled fiber holders with a movement resolution of 0.02 μm in the lateral direction and 0.25 μm along the fiber axis. The filament loop is driven by electrical current and the fiber is heated to its softening point in a very repeatable and controllable manner. In our experiment the filament power was set at 20 W with a heating duration of 5.35 s.

Figure 2 shows microscope images of the lateral offset splicing process, before (a) and after (b) splicing. The fiber ends are initially positioned with an axial spacing of 8.0 μm and a lateral misalignment of 19.5 μm. To ensure a strong mechanical splice under such large lateral offset during the heating process, both ends are pushed toward each other with a total distance of 12 μm. Using resistive heating and axial compression, we achieve a mechanically robust splice with a core to core misalignment of 7.8 μm. Unlike conventional fusion splicers, the Vytran GPX-3400 microscope illuminates through the fiber, allowing the fiber cores to be observed. Close examination of the spliced joint shows that the two terminated cores are bent away from each other in such a way that there is no overlap of the two cores at the join. In fact, we would expect that light propagating along either core towards the join will couple strongly to the cladding on the other side of the join, and only weakly to the opposite core. The core deflection on either side of the spliced joint is due to the initial lateral misalignment of the fibers followed by 4 μm overlapping (we push 12 μm for an initial fiber end facet separation of 8 μm) of the fibers during the fusion process. This yields a mechanically robust splice with a smooth offset curve along the fiber cladding surface due to the surface tension.

3. Experiment and discussion

As seen in Fig. 3, the reflection spectrum changes according to the amount of lateral offset in the splice. With no offset, the spectrum is dominated by a single Bragg resonance. With small offset of 1.6 μm, the core mode is weakened by about 3 dB (because the light passes twice through the lossy misaligned core joint) and there is a prominent ghost resonance caused by the recoupling of low order cladding modes between 1549 and 1551 nm and a slight hint of a higher order cladding mode feature between 1544 and 1549 nm. For the high core offset of 7.8 μm, we see a 10 dB decrease in the core mode feature (again caused by the lossy core to core coupling), a further increased low order cladding mode (ghost resonance) feature, and a much broader and stronger high order cladding mode feature caused by the generation by the tilted grating and recapturing of the high order cladding mode light by the upstream fiber core.
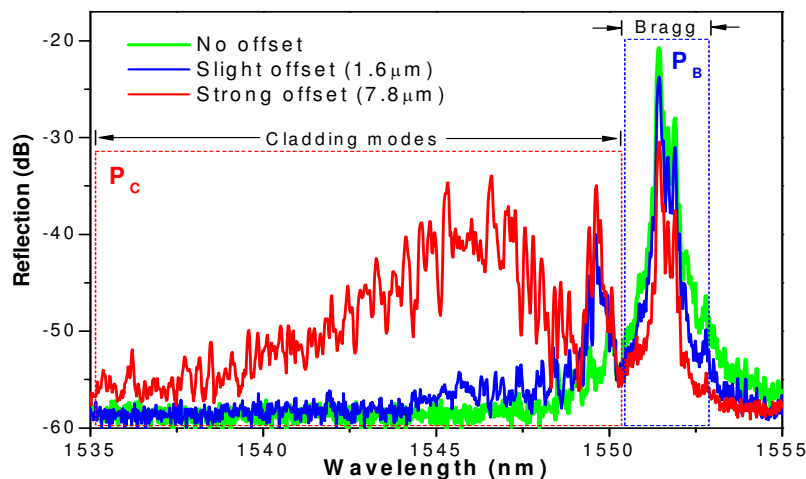

Fig. 3. Reflection spectra of TFBG (6°) before and after misaligned splicing, where the slight offset and strong offset correspond to the core-core misalignment of 1.6 μm and 7.8 μm, respectively, after splicing.

We discuss the behaviour of modes in this structure both before and after the light are recoupled into the core at the offset core junction. Before the cladding modes recouple back to the fiber core, their behavior is essentially guided by the cladding boundary, as their effective

index depends on the refractive index of the surrounding medium. The sensitivity of the cladding-mode effective index to the external index increases with mode order since the radial extent of the evanescent field increases for higher-order modes (i.e. those with shorter wavelengths). Therefore, when the SRI increases, the higher-order cladding modes are first affected and eventually lost by radiation from the fiber cladding [19]. With the SRI increasing further, more and more cladding modes gradually become affected until only two dominating peaks remain: the ghost modes (which corresponds to a group of strongly guided cladding modes that interact little with the cladding boundary) and residual core-mode (Bragg resonance). The lateral-offset fused joint functions as a bridge between the core and cladding and the above changes of cladding-modes are visible in the light eventually extracted from the upstream fiber's core. Once such cladding modes are coupled into the fiber core, they are no longer affected by the SRI of the connecting fiber between the sensor and the interrogator and the SRI around the TFBG can be unambiguously determined. Figure 4 shows the reflection spectra of the TFBG for five values of SRI. We show in the next section that this change is monotonic over a large range of SRI. Therefore, the SRI can be unambiguously determined by reflected power measurement.
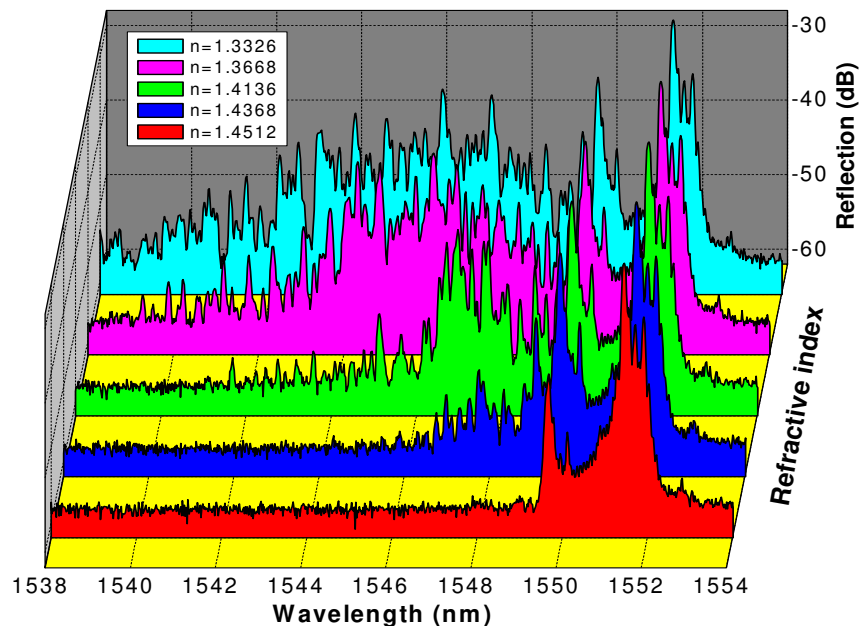

Fig. 4. Spectral response of TFBG versus SRI.

We constructed a sensor as described in section 2, using a one centimeter-long fiber Bragg grating with a tilt angle of 6° inscribed in hydrogen-loaded Corning SMF-28 fiber using a pulsed KrF excimer laser and a phase mask. We launched light from an erbium doped fiber amplified spontaneous emission broadband source into the sensing fiber through a 3 dB coupler. The core mode and cladding mode reflected powers from the sensor were monitored by two photodiodes in conjunction with two bandpass filters, the details of which are described below. To keep the fiber stationary during the experiments, we secured the grating on to a microscope slide. Small quantities of liquids with various refractive indices were dispensed with a pipette onto the grating. A second slide was used to cover the interaction region and to maintain the liquid in place by capillary action. The immersion liquids used were sucrose-water solutions providing a range of RI from 1.33 to 1.46. The refractive indices of the solutions were measured at a wavelength of 589 nm with an Abbe refractometer.

The cladding waves in silica fiber, which has a refractive index of about 1.46, are strongly guided when the surrounding refractive index is much lower than 1.46 and thus reduces the interaction between the cladding wave and its surrounding. As a result, most types of

evanescent field based fiber refractometers (FBG [5], TFBG [10], LPG [13]) have rapidly diminishing sensitivities for SRI values less than 1.4, limiting their usefulness in most biochemical applications. However, the reflection spectra in Fig. 4 show that the proposed sensor is sensitive to index changes down to 1.33. Obvious spectral change within the wavelength band of 1538 - 1542 nm was observed for slight SRI changes from 1.33 (blue profile) to 1.36 (pink profile)). With the SRI increasing further, more cladding modes become affected showing a large spectrum decrease from the short wavelength side, until only the ghost and Bragg resonance remain. Because of the large sensitivity of high order cladding mode to the low SRI, slight changes in the refractive index of water or water-based solutions can be identified by bandpass filtering the reflected power of the concerned band.
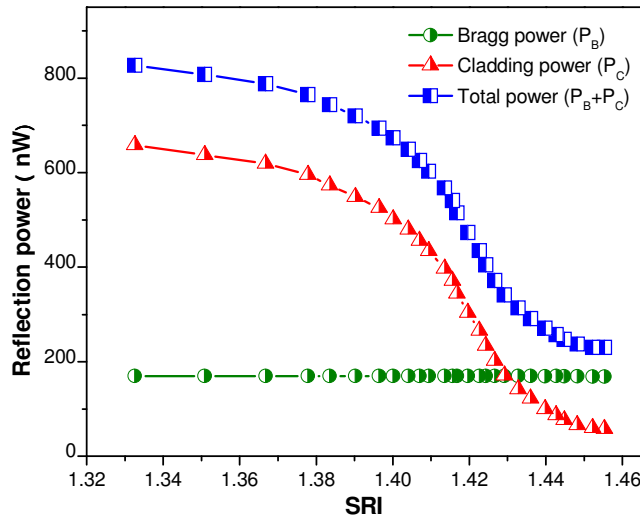

Fig. 5. TFBG reflection power versus SRI, with separate power detection for the core-guided Bragg reflected mode (P_B) and the recoupled cladding modes (P_C).
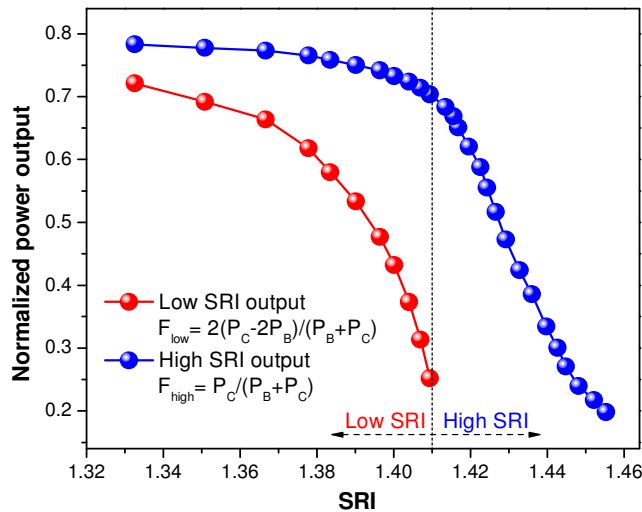

Fig. 6. Normalized power output for SRI measurement with an improved sensitivity in lower SRI.

Changes in refractive index of the surrounding medium are monotonically related to the optical power in particular wavelength bands. In Fig. 5, we plot the optical power in the two wavelength bands, as a function of the SRI. The bands were chosen to include different

groups of modes: The power in the Bragg reflected core mode, P_B, was measured from 1551 nm to 1553 nm, while the power in the cladding modes, P_C, was measured from 1535 nm to 1551 nm. We see that, as expected, the core mode is insensitive to surrounding refractive index, while the cladding modes are sensitive. Even at the refractive index of 1.33, the measured sensitivity was 1100 nW/u.r.i. (u.r.i. stands for "units of refractive index"), where the noise power of the sensing system is less than 10 nW. We can therefore detect a small change in low SRI by detecting the reflected power change of the concerned high order cladding resonances using a selected bandpass filter.

Compared to the longer-wavelength-side Bragg resonance, power contained in high order cladding modes is smaller (10 dB or even more). We introduce two normalization functions, $F_{low} = 2(P_C - 2P_B)/(P_B + P_C)$ and $F_{high} = P_C/(P_B + P_C)$, to conveniently emphasize low- and high-SRI measurements, respectively. Here, P_B works as a power reference, as it is not sensitive to the SRI change and provides an effective calibration of any possible power variations caused by the instability of the light source and the connecting loss. As Fig. 6 shown, the two normalized functions F_{low} and F_{high} provide a high normalization sensitivity (20~80 %) and a monotonic response in a large dynamic SRI range, functioning as a refractometer for both high SRI and low SRI. In a future development, we propose to increase the refractometer's sensitivity at lower values of SRI by dividing the cladding mode band into two or more narrower wavelength bands with separated power monitoring.

4. Conclusion

A novel and simple reflective fiber grating-based refractometer for measuring surrounding refractive index as low as 1.33 has been presented and demonstrated experimentally. The sensor comprises a weakly tilted FBG, that is fusion spliced with a large lateral offset to a piece of standard singlemode fiber. The interrogation of the sensor only requires a 3 dB-coupler, two relatively coarse bandpass filters and two photodetectors. The self-referenced core mode detection (independent of SRI) provides a normalization signal that is proportional to the light source power and therefore cancelled out possible power fluctuations. The sensor works in reflection and the length of the entire sensor "head" can be very small (as little as 10 to 20 mm). Because of its sensitivity to refractive index as small as 1.33, the new sensor shows great potential for aqueous chemical and biological applications.

Acknowledgments